



Photoinduced Electron Transfer from Imidazole Derivative to Nano Semiconductors : New Approach

N. Srinivasan*

Department of Chemistry, S.K.P.Engineering College, Thiruvanamalai, TN, India.

Received : 16.02.2013 Revised : 04.03.2013 Accepted : 16.03.2013

Abstract

Bioactive imidazole derivative absorbs in the UV region at 305 nm. The interaction of imidazole derivative with nanoparticulate WO_3 , Fe_2O_3 , Fe_3O_4 , CuO , ZrO_2 and Al_2O_3 has been studied by UV-visible absorption, FT-IR and fluorescence spectroscopies. The imidazole derivative adsorbs strongly on the surfaces of nanosemiconductor, the apparent binding constants for the association between nanomaterials and imidazole derivative have been determined from the fluorescence quenching. In the case of nanocrystalline insulator, fluorescence quenching through electron transfer from the excited state of the imidazole derivative to alumina is not possible. However, a possible mechanism for the quenching of fluorescence by the insulator is energy transfer, that is, energy transferred from the organic molecule to the alumina lattice. Based on Forster's non-radiation energy transfer theory, the distance between the imidazole derivative and nanoparticles ($r_0 \sim 2.00$ nm) as well as the critical energy transfer distance ($R_0 \sim 1.70$ nm) has been calculated. The interaction between the imidazole derivative and nanosurfaces occurs through static quenching mechanism. The free energy change ($-G_{ct}$) for electron transfer process has been calculated by applying Rehm-Weller equation.

Keywords : Association constant ; Electron transfer; Imidazole; Nanoparticles; Quenching.

1. INTRODUCTION

Nanocrystalline semiconductors with unique properties such as large surface area, pore structure, embedded effect and size effect are recognized to have potential applications in electronics, optics, genomics, proteomics and bioanalytical fields. The combination of nanoparticles and biological molecules has attracted tremendous attention, where nanoparticles could present a versatile nanoscale interface for biomolecular recognition (Moyano et al. 2011). Some researchers have reported the specific interaction between nanoparticles and protein as well as other biomolecules (Graeme et al. 2010). A new direction has emerged in potential biotechnological applications such as luminescence tagging, immunoassay, drug delivery and

cellular imaging (Alivisatos et al. 1996). The electron-transfer process at the semiconductor-dye interface has been successfully utilized in the development of solar cells, electronic devices, heterogeneous photo catalysis and waste water treatment (Higashitani et al. 2011). The efficiency of these processes depends on the properties of the sensitizers, semiconductor and their interaction under photo excitation. Recently, semiconductor composite nanostructures have become an attractive topic because of their potential applications in different fields (Li et al. 2009).

Heterocyclic imidazole derivatives have attracted considerable attention because of their unique optical properties and used for preparing functionalized materials. Benzimidazole based chromophores have received increasing attention due to their distinctive linear, non-linear optical properties and also due to their excellent thermal stability in guest-host systems.

*N.Srinivasan Tel.:+91 9865768426

E-mail : sreene2008@gmail.com

Arylimidazole derivatives play important role in materials science due to their optoelectronic properties (Jean-François Lefebvre et al. 2010). They are used as ligands for the synthesis of metal complexes of ruthenium(II), copper(II), cobalt(II), nickel(II), manganese(II), iridium(III) and several lanthanides for nonlinear optical (NLO) applications.

They are important building blocks for the synthesis of proton, anion and cation sensors. The fluorescence quenching technique is applied to study the interaction between nanomaterials and imidazole derivative to infer the association and also the energy transfer between them (Scheme S1). According to the plot of $\log [(F_0 - F)/F]$ versus $\log [Q]$, the binding constants have been determined. Further, the mechanism of electron transfer process on the basis of energy level diagram has also been proposed in this paper. Distance between the imidazole derivative and nanosurfaces ($r_0 \sim 2.00$ nm) as well as the critical energy transfer distance ($R_0 \sim 1.70$ nm) has also been calculated (Jayabharathi et al. 2011).

2. MATERIALS AND METHODS

2.1. Materials

Butane-2,3-dione (Sigma--Aldrich Ltd.), *p*-toluidine, benzaldehyde and all other reagents have been purchased from S.D. fine chemicals and used without further purification. The nanoparticles used were those supplied by Sigma-Aldrich Ltd. and characterized (Karunakaran et al. 2011); the average crystal size (D) and surface area (S) are listed in Table 1.

2.2. Measurements

The ^1H and ^{13}C NMR spectra of the ligand have been recorded on a Bruker 500 MHz NMR instrument. Mass spectrum was recorded using Agilent 1100 mass spectrometer. The fluorescence quenching measurements have been carried out using a Perkin Elmer LS55 spectrofluorimeter. The excitation wavelength was 304 nm and the emission was monitored at 362 nm. The excitation and emission slit widths (each 10 nm) and scan rate (600 nm min^{-1}) were kept constant for all the measurements. The samples were deoxygenated by

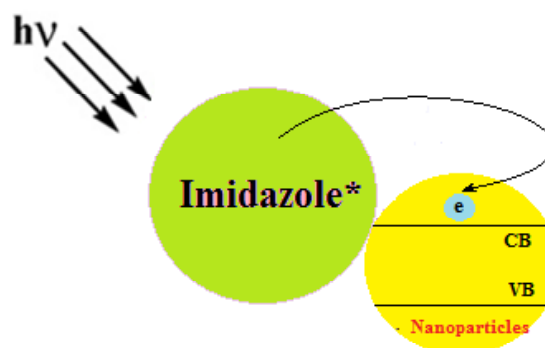
bubbling with pure nitrogen gas. The absorption spectral measurements were recorded by using a Perkin Elmer Lambda 35 spectrophotometer. An ethanolic solution of the imidazole derivative of required concentration ($1 \times 10^{-8} \text{ M}$) was mixed with nanoparticles dispersed in ethanol at different loading and the absorbance and emission spectra were recorded. The nanocrystals were dispersed under sonication in ethanol using ethylene glycol followed by dilution with ethanol.

2.3. Synthesis of the imidazole derivative

The experimental procedure used was the same as described in our recent papers (Jayamoorthy et al. 2013) The imidazole derivative was synthesized by four components assembling of Butane-2,3-dione (40 mmol), *p*-toluidine (30 mmol) ammonium acetate (30 mmol) and benzaldehyde (30 mmol). The four components were refluxed in ethanol for 24 h at 80°C . The reaction mixture was extracted with dichloromethane and purified by column chromatography using hexane-ethyl acetate (9:1) as the eluent.

2.3.1 4,5-Dimethyl-1-(*p*-methylphenyl)-2-phenyl-1H-imidazole

Yield: 40%. m.p. 125°C . ^1H NMR (400 MHz, CDCl_3): δ 2.02 (s, 3H), 2.31 (s, 3H), 2.42 (s, 3H), 7.02-7.36 (aromatic protons). ^{13}C NMR (100 MHz, CDCl_3): δ 9.57, 12.76, 21.19, 125.45, 127.54, 127.63, 127.97, 128.01,



Scheme S1. : Photoinduced charge injection and charge separation.

130.11, 130.92, 133.41, 135.34, 138.37, 145.15. MS: m/z 260.00, calcd. 262.35.

3. Results and discussion

3.1. Absorption characteristics of imidazole derivative–nanoparticles

The absorption spectra of imidazole derivative in presence of nanoparticles dispersed at different loading and also in their absence are displayed in Fig. 1. The nanoparticles enhance the absorbance of imidazole derivative remarkably without shifting its absorption maximum (304 nm). This indicates that the nanocrystals do not modify the excitation process of the ligand. The enhanced absorption at 304 nm observed with the dispersed semiconductor nanoparticles are due to adsorption of the imidazole derivative on semiconductor surface. This is because of effective transfer of electron from the excited state of the imidazole derivative to the conduction band of the semiconductor nanoparticles. However, this inference is not applicable to alumina; alumina is an insulator and the possible explanation is energy transfer from the excited state of the ligand to the alumina lattice.

3.2. FT-IR characteristics of imidazole derivative–nanoparticles

The UV-visible absorption spectroscopy is not sufficient to throw light on the molecular structure of imidazole derivative adsorbed on surfaces of nanoparticles and Fourier transform infrared (FT-IR) technique may provide further information about the nature of interaction between the organic molecule and the inorganic surfaces. The spectrum of pure imidazole derivative shows the >C=N stretching vibration at 1596 cm⁻¹. This band is shifted in imidazole derivative bound to nanoparticle; a new band appears at 1622 cm⁻¹ in place of 1596 cm⁻¹. These observations show that the imidazole derivative is adsorbed on the surface of nanoparticles.

3.3. Fluorescence quenching characteristics

Fig. 2 displays the effect of increasing concentration of nanoparticles on the fluorescence

emission spectrum of imidazole derivative. Addition of nanoparticles to the solution of imidazole derivative resulted in the quenching of its fluorescence emission. This quenching behavior is similar to the studies reported earlier (Zhou et al. 2002) The apparent association constants (K_{app}) have been obtained from the fluorescence quenching data using the following equation

$$1/(F_0 - F) = 1/(F_0 - F) + 1/K_{app} (F_0 - F) \quad (1)$$

[nanoparticles]

where K_{app} is the apparent association constant, F_0 is the initial fluorescence intensity of the imidazole derivative, F is the fluorescence intensity of the imidazole derivative adsorbed on nanoparticles and F is the observed fluorescence intensity at its maximum. A good linear relationship between $1/(F_0 - F)$ and the reciprocal concentration of nanoparticles is seen. From the slope, the values of apparent association constants (K_{app}) have been assessed for imidazole derivative–nanoparticles.

The fluorescence quenching behavior is usually described by Stern–Volmer relation:

$$I_0/I = 1 + K_{sv} [Q] \quad (2)$$

where, I_0 and I are the fluorescence intensities in the absence and presence of quencher, K_{sv} is the Stern–Volmer constant related to the bimolecular quenching rate constant and Q is the quencher. Addition of nanoparticles to a solution of imidazole derivative results in quenching of fluorescence emission. Typical linear S–V plot for steady-state fluorescence quenching of imidazole derivative by nanoparticles is shown in Fig. 3.

The ability of the excited state imidazole derivative to inject its electrons into the conduction band of nanoparticles is determined from the energy difference between the conduction band of nanoparticles and excited state oxidation potential of imidazole derivative. According to the equation $E_{s^*/s^+} = E_{s/s^+} - \Delta E_s$, the oxidation potential of excited singlet state imidazole derivative is 3.10 V (vs. NHE), where, E_{s/s^+} is the oxidation potential of imidazole derivative, 0.14 V (vs. NHE) and E_s is the excited state energy, 3.25 eV; the excited state energy of

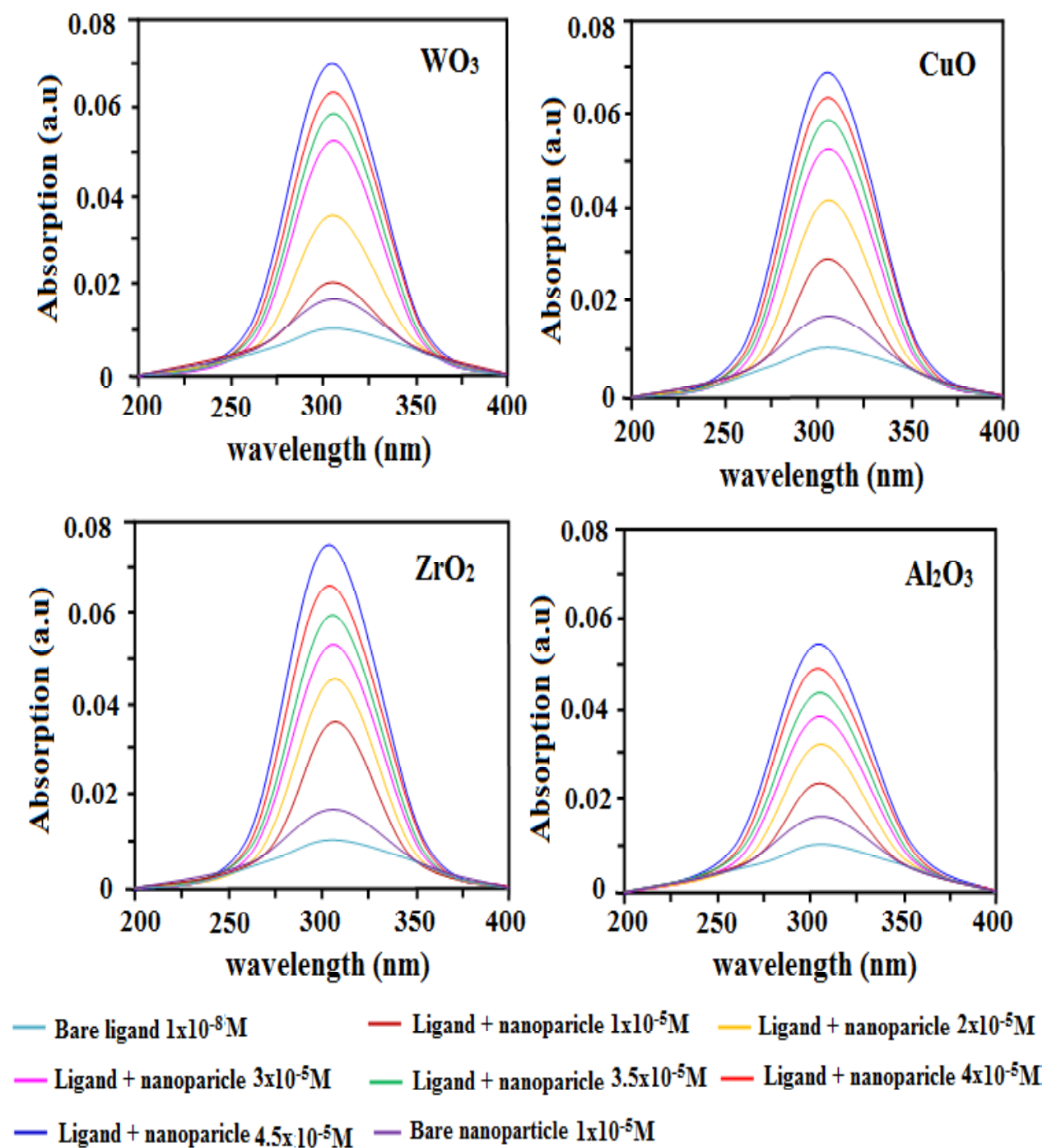


Fig.1 : Absorption spectra of imidazole derivative in presence and absence of nanoparticles.

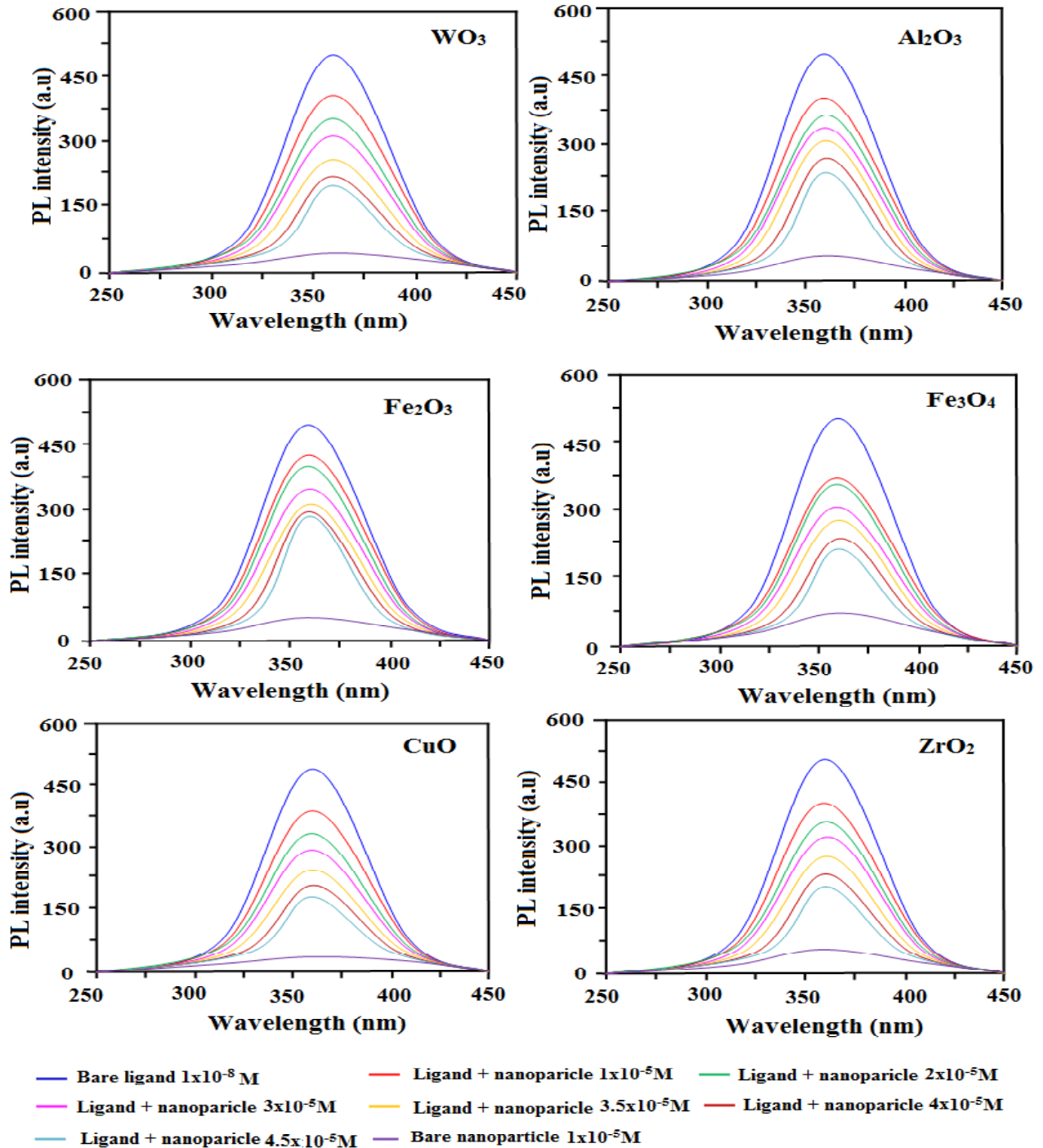


Fig.2 : Fluorescence quenching of imidazole derivative in the presence and absence of various concentrations of nanoparticles

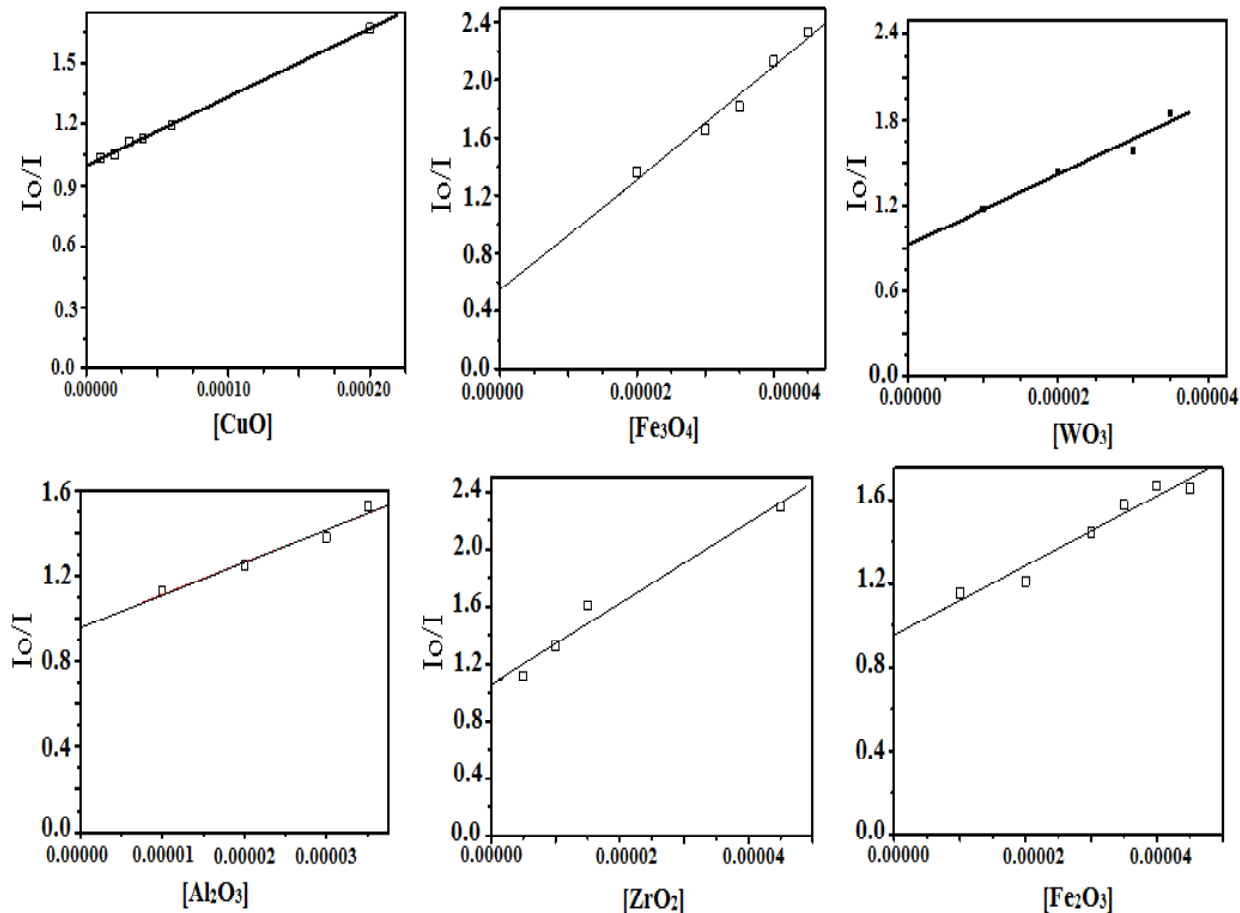


Fig.3 : Stern-Volmer plot of fluorescence quenching of imidazole with various concentrations of nanoparticles.

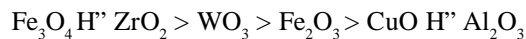
the imidazole derivative is calculated from the fluorescence maximum based on the reported method (Shin et al. 2002).

3.4. Binding constant and number of binding sites

Static quenching arises from the formation of complex between fluorophore and the quencher and the binding constants (K) have been calculated by using the equation

$$\log [(F_0 - F)/F] = \log K + n \log [Q] \quad (3)$$

where K is the binding constant of nanoparticles with imidazole derivative, which can be determined from the intercept of $\log [(F_0 - F)/F]$ versus $\log [Q]$ as shown in Fig. 4 and the calculated value of binding constant K and number of binding sites (n) are given in Table 2. The order of binding constant K is



The value of “ n ” is close to unity which indicates single binding of the organic molecule to the nanoparticulate surface. The observed low binding of imidazole derivative with alumina is because of absence

of electron transfer. Alumina is an insulator and the observed quenching is due to energy transfer. That is, energy transferred from the excited organic molecule to the alumina lattice. It is well known that energy transfer is less efficient than electron transfer. The large binding constant observed with Fe_3O_4 is due to the large energy difference between the excited state of imidazole derivative and the conduction band edge of Fe_3O_4 . Similar explanation is valid for WO_3 . The conduction band edges of Fe_2O_3 and CuO do not differ largely and so are the

binding constants. However, the binding constant with zirconia is as large as that with Fe_3O_4 but the energy difference is not as large as that of Fe_3O_4 . A possible explanation for the observed surprising results with zirconia is that it is a well known heterogeneous catalyst (Madje et al. 2004) Further, the quenching of fluorophore of the imidazole derivative by nanoparticle may also be due to the binding of the fluorophore of the organic molecule with the nanoparticulate semiconductors (Scheme S2).

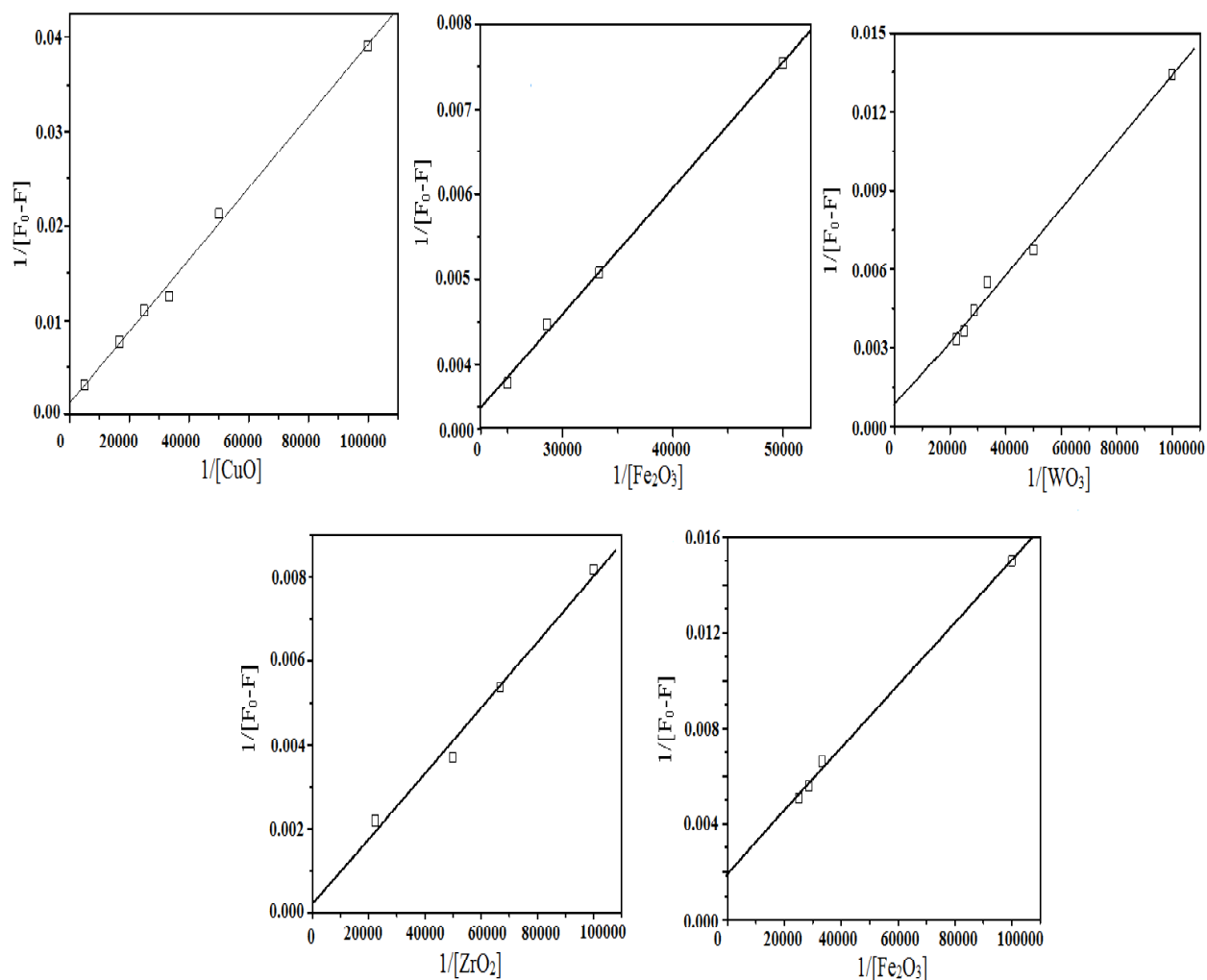
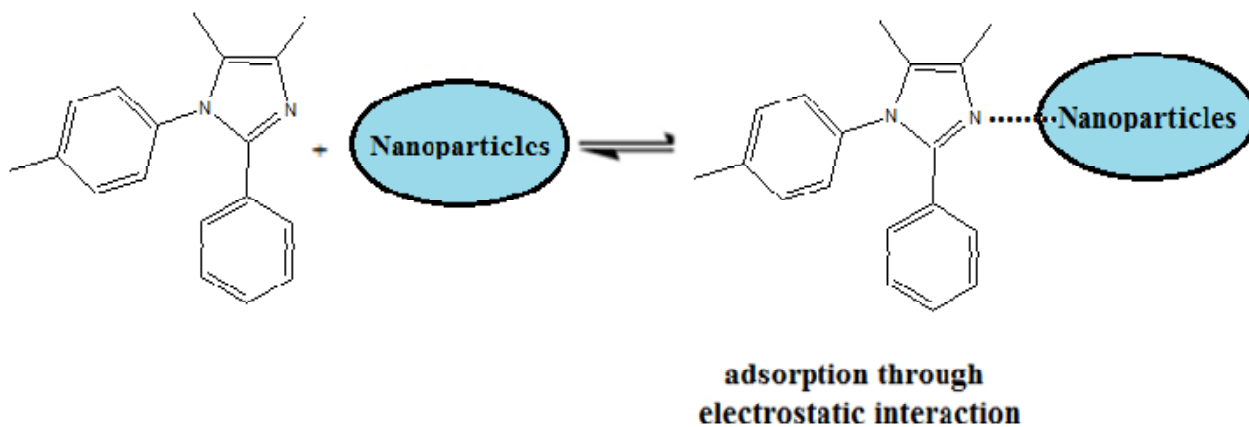


Fig.4 : Plot of $1/(F_0 - F)$ versus $1/[Q]$.



Scheme S2. Schematic diagram describing the electron-donating energy level of imidazole

3.5. Energy transfer between nanoparticles and imidazole derivative

The decrease in fluorescence intensity is attributed to electron transfer between imidazole derivative and the nanoparticles in the case of semiconductors and energy transfer in the case of insulator. The excited state energy of the imidazole derivative is larger than the conduction band energy levels of nanosemiconductors (Lin et al. 1991). This makes possible the energy transfer from the excited state of imidazole derivative to the nanoparticles.

Energy transfer efficiency (E) is given by the following equation:

$$E = 1 - (I/I_0) \quad (4)$$

where, I is the emission intensity of donor in the presence of acceptor and I_0 is the emission intensity of the donor alone. From the above results it is clear that, in presence of nanoparticles, the fluorescence intensity of imidazole derivative is reduced (from I_0 to I) by energy transfer to nanoparticles.

According to Forster's non-radioactive energy transfer theory, the energy transfer efficiency is related not only to the distance between the acceptor and donor (r_0), but also to the critical energy transfer distance

(R_0) (Table 3). That is

$$E = R_0^6 / (R_0^6 + r_0^6) \quad (5)$$

where, R_0 is the critical distance when the transfer efficiency is 50%.

$$R_0^6 = 8.8 \times 10^{-25} K^2 N^{-4} \phi J \quad (6)$$

where, K^2 is the spatial orientation factor of the dipole, N is the refractive index of the medium, ϕ is the fluorescence quantum yield of the donor and J is the overlap integral of the fluorescence emission spectrum of the donor and the absorption spectrum of the acceptor (Fig.5). The value of J can be calculated by using Eq. (7),

$$J = \int F(\lambda)\epsilon(\lambda)\lambda^4 d\lambda / \int F(\lambda)d\lambda \quad (7)$$

where, $F(\lambda)$ is the fluorescence intensity of the donor, $\epsilon(\lambda)$ is molar absorptivity of the acceptor. The parameter J can be evaluated by integrating the spectral parameters in Eq. (7). Under these experimental conditions, the value of R_0 calculated from Eq. (6) is found to be about 1.70 nm in all cases; the values of K^2 ($= 2/3$) and N ($= 1.3467$) used are from the literature (Cyril et al] and the ϕ value ($= 0.15$) is from the present study. Obviously, the calculated value of R_0 is in the range of maximal critical distance (Chen et al. 1990). This is in accordance with the conditions of Forster's non-radiative energy transfer

theory, indicating the static quenching interaction between nanoparticles and imidazole derivative. The value of r_0 obtained using Eq. (4) is less than 8 nm. This suggests that non-radioactive energy transfer occurs

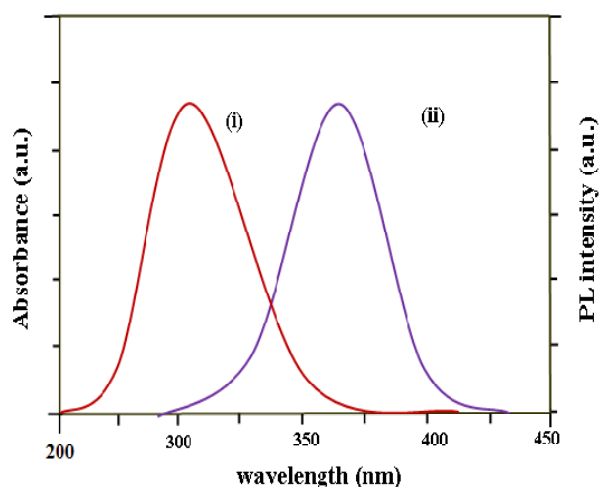


Fig.5 : Overlapping of fluorescence and absorption spectra of donor and acceptor.

between the nanoparticles and imidazole derivative with high probability (He et al. 2005) The fact that the value of r_0 is larger than that of R_0 in the present study also reveals the operation of static-type of quenching mechanism (Hu et al. 2005) Furthermore, it is suggested that the binding of nanoparticles and imidazole derivative occurs through energy transfer.

3.6. Calculation of free energy change (ΔG_{et}) for electron transfer process]

The thermodynamic feasibility of excited state electron transfer reaction has been confirmed by the calculation of free energy change by employing the well known Rehm-Weller expression (Kavarnos et al. 1986)

$$\Delta G_{et} = E^{1/2}_{(ox)} \Delta E^{1/2}_{(red)} \Delta E_s + C \quad (8)$$

where, $E^{1/2}_{(ox)}$ is the oxidation potential of imidazole derivative (0.14 V), $E^{1/2}_{(red)}$ is the reduction potential of

nanoparticles, that is, the conduction band potential of nanoparticles, E_s is the excited state energy of imidazole derivatives and C is the coulombic term. Since one of the species is neutral and the solvent used is polar in nature, the coulombic term in the above expression can be neglected (Parret et al. 1994). The values of " G_{et} " are calculated as "2.43 eV (Al_2O_3), "2.43 eV (WO_3), "2.83 eV (Fe_2O_3), "1.88 eV (Fe_3O_4), "2.65 eV (CuO) and "4.20 eV (ZrO_2). The high negative values indicate the thermodynamic feasibility of the electron transfer process (Kikuchi et al. 1993).

4. CONCLUSION

Imidazole derivative is adsorbed on the surfaces of semiconductor nanoparticles through azomethine nitrogen. The conduction band energy positions determine the electron transfer from excited state imidazole derivative to the nanoparticles. The distances between the imidazole derivative and nanoparticles, deduced on the basis of Forrester's non-radiation energy transfer theory are close to 2.0 nm and the critical energy transfer distances are found to be about 1.70 nm. The negative ΔG_{et} values for all nanoparticles reveal that the electron transfer process is thermodynamically favorable. Quenching of fluorescence by nanoparticulate alumina is most likely due to energy transfer.

REFERENCES

- Alivisatos, A., Semiconductor Clusters, Nanocrystals, and Quantum Dots, *Science*, 271, 933-937 (1996).
- Chen, G.Z., Huang, X.Z., Xu, J.G., Wang, Z.B. and Zhang, Z.Z., Method of fluorescent Analysis, second ed., Science Press, Beijing, 1990, 123, 126 (Chapter 4).
- Cyril, L., Earl, J.K. and Sperry, W.M., Biochemists Handbook, E & F.N. Spon, London, 1961.
- He, W.Y., Li, Y., Xue, C.X., Hu, Z.D., Chen, X.G. and Sheng, F.L., Effect of Chinese medicine alpinetin on the structure of human serum albumin, *Bioorg Med Chem.*, 13, 1837 (2005).
- Hu, Y.J., Liu, Y. and Zhang, L.X., Studies of interaction between colchicine and bovine serum albumin by fluorescence quenching method, *J Mol Struct.*, 750, 174 -178 (2005).

- Hu, Y.J., Liu, Y. and Zhang, L.X., Studies of interaction between colchicine and bovine serum albumin by fluorescence quenching method, *J Mol Struct.*, 750, 174 -178 (2005).
- Hunter, K., Jason O'Young., Bernd Grohe., Mikko Karttunen. and Goldberg, A., The Flexible Polyelectrolyte Hypothesis of Protein-Biomineral Interaction, *Langmuir*, 26, 18639–18646 (2010).
- Jayabharathi, J., Thanikachalam, V., Saravanan, K. and Srinivasan, N., Iridium(III) complexes with orthometalated phenylimidazole ligands subtle turning of emission to the saturated green colour, *J Fluoresc.*, 21, 507-519 (2011).
- Jayamoorthy, K., Mohandas, T., Sakthivel, P. and Jayabharathi, J., 1-Phenyl-2-[4-(trifluoromethyl)phenyl]-1H-benzimidazole, *Acta Cryst.*, E69, o244 (2013)
- Jean-François Lefebvre., Dominique Leclercq., Jean-Paul Gisselbrecht. and Sébastien Richeter., Synthesis, Characterization, and Electronic Properties of Metalloporphyrins Annulated to Exocyclic Imidazole and Imidazolium Rings, *Eur J Org Chem.*, 2010, 1912–1920(2010).
- Karunakaran, C., Anilkumar, P. and Gomathisankar, P., Photo production of iodine with nanoparticulate semiconductors and insulators, *Chem Cent J.*, 123, 5:31(2011).
- Kavarnos, G.J. and Turro, N.J., Photosensitization by reversible electron transfer: theories, experimental evidence, and examples, *Chem Rev.*, 86, 401–449 (1986).
- Kikuchi, K., Niwa, T., Takahashi, Y., Ikeda, H. and Miyashi, T., Quenching mechanism in a highly exothermic region of the Rehm-Weller relationship for electron-transfer fluorescence quenching, *J Phys Chem.*, 97, 5070–5073 (1993).
- Ko Higashitani., McNamee, E. and Masaki Nakayama., Formation of Large-Scale Flexible Transparent Conductive Films Using Evaporative Migration Characteristics of Au Nanoparticles, *Langmuir*, 27, 2080–2083(2011).
- Li, J. and Zhang, Z., Optical properties and applications of hybrid semiconductor nanomaterials, *Coord Chem Rev.*, 253, 3015-3041(2009).
- Lin, B., Fu, Z. and Ji, Y., Green luminescent center in undoped zinc oxide films deposited on silicon substrates, *Appl Phy Lett.*, 79, 943-945 (1991).
- Madje, B.R., Patil, P.T., Shindalkar, S.S., Benjamin, S.B., Shingare, M.S. and Dongare, M.K., Facile transesterification of β -ketoesters under solvent-free condition using borate zirconia solid acid catalyst, *Catal Commun.*, 5, 353–357 (2004).
- Moyano, F. and Rotello, M., Nano Meets Biology: Structure and Function at the Nanoparticle Interface, *Langmuir*, 27, 10376–10385 (2011).
- Parret, S., Savary, F.M., Fouassier, J.P. and Ramamurthy, P., Spin—orbit-coupling-induced triplet formation of triphenylpyrylium ion: a flash photolysis study, *J Photochem Photobiol A: Chem.*, 83, 205–209 (1994).
- Shin, E.J. and Kim, D., Substituent effect on the fluorescence quenching of various tetraphenylporphyrins by ruthenium tris(2,22 -bipyridine) complex, *J Photochem Photobiol A: Chem*, 152, 25–31 (2002).
- Zhou, Z., Qian, S., Yao, S. and Zhang, Z., Electron transfer in colloidal TiO₂ semiconductors sensitized by hypocrellin A, *Radiat Phys Chem.*, 65, 241–248 (2002).

Publishers, Advisory/Editorial Board/Editor-in-Chief take no responsibilities for inaccurate, misleading data, opinion and statement appeared in the articles published in this Journal. All responsibilities of the content rest upon the corresponding author.